



2nd International Conference on Structural Integrity, ICSI 2017, 4-7 September 2017, Funchal, Madeira, Portugal

On strength analysis of highly porous materials within the framework of the micropolar elasticity

Victor A. Eremeyev^{a*}, Andrzej Skrzat^a, Feliks Stachowicz^a, Anastasia Vinakurava^a

^a*Rzeszow University of Technology, 35959 Rzeszów, Poland*

Abstract

We discuss the finite element approach to modelling of static deformations of porous materials such as foams, beam lattices, and others within the linear micropolar elasticity. It is known that the micropolar elasticity may be used for microstructured solids and fluids since it can forecast size-effect near geometrical singularities such as holes, notches, small contact areas of two solids. Within the micropolar elasticity the translational and rotational interactions of the material particles can be taken into account. Here we present the recent developments in the theory of finite elements calculations for micropolar solids in order to capture the stress behaviour in the vicinity of geometric singularities such as holes, notches, imperfections or contact areas. The fundamental equations of the micropolar continuum are presented. The FEM implementation in micropolar elasticity is given. The new 8-node hybrid micropolar isoparametric element and its implementation in ABAQUS are introduced. The solutions of few 3D benchmark problems of the micropolar elasticity are given. Among them are analysis of stresses and couple stresses near notches and holes, contact problem of parabolic stamp and half space. The main attention is paid to modelling of interaction between a biodegradable porous implant and a trabecular bone. Comparison of classical and micropolar solutions is carefully discussed. Comparison of classical and micropolar solutions is discussed. Numerical tests have shown that couple stress appears almost in the vicinity of geometrical singularities. It is shown that micropolar elasticity allows to obtain better results for domains with microstructures and singularities than classical theory of elasticity.

© 2017 The Authors. Published by Elsevier B.V.

Peer-review under responsibility of the Scientific Committee of ICSI 2017

Keywords: micropolar elasticity; finite element method; foams; porous materials; bones

* Corresponding author. Tel.: +0-000-000-0000 ; fax: +0-000-000-0000 .

E-mail address: veremeyev@prz.edu.pl

1. Introduction

Nowadays the interest grows to generalized models of continuum in order to model complex behavior of such microstructured materials as foams, bones and other porous and cellular materials. Among many generalized model the micropolar elasticity plays an important role, see Eringen (1999), Eremeyev et al. (2013). It can capture size-effect well-established for nanomaterials (Liebold and Müller (2015)), it also inherits rotational interactions and moments used in structural mechanics, see Goda and Ganghoffer (2015). The micropolar elasticity was proposed by Cosserat brothers more than hundred years ago and also found many applications for modeling of such materials as masonries, magnetic fluids, composites, etc., see Yang and Lakes (1982), Lakes (1986), Trovalusci et al. (2015), Eremeyev and Pietraszkiewicz (2012), Eremeyev et al. (2013). Within the micropolar elasticity two kinematically independent fields of translations and rotations and the stress and couple stress tensors are introduced.

Effective solution of boundary-value problems for micropolar solids requires development of advanced numerical code such as the finite element method and its implementation in efficient software. In particular, some commercial FEM software gives the possibility to use extended model of continuum applying so-called user defined elements and user defined material procedures. Here we discuss the implementation of new micropolar finite elements in ABAQUS.

2. Governing Equations of the Linear Micropolar Elasticity

Following Eringen (1999), Eremeyev et al. (2013). we recall the basic equations of the linear micropolar elasticity. For simplicity we restrict ourselves by isotropic solids. The kinematic of a micropolar solid is described by two fields that are the field of translations u_i and the field of rotations θ_i , $i=1,2,3$. The latter is responsible for the description of moment (rotational) interactions of the material particles. Hereinafter the Latin indices take on values 1, 2, or 3 and we use the Einstein summation rule over repeating indices. The equilibrium equations take the form

$$t_{ji,j} + f_i = 0, \quad m_{ji,j} + e_{imn}t_{mn} + c_j = 0, \quad (1)$$

where t_{ij} and m_{ij} are the Cartesian components of the nonsymmetric stress and couple stress tensors, respectively, e_{ijk} is the permutation symbol (Levi-Civita third-order tensor), and f_j and c_j are external forces and couples. Notation $a_{,j}$ means the partial derivative of a with respect to Cartesian coordinate x_j .

The static and kinematic boundary conditions have the following form

$$n_i t_{ij} |_{A_i} = \phi_j, \quad n_i m_{ij} |_{A_i} = \eta_j, \quad u_i |_{A_u} = u^0_i, \quad \theta_i |_{A_u} = \theta^0_i, \quad (2)$$

where n_i is the components of the external normal to the boundary $A = A_i \cup A_u$, ϕ_j and η_j are external forces and couples prescribed on A_i , and u^0_i and θ^0_i are given on A_u surface fields of translations and rotations, respectively.

Within the linear Cosserat continuum the constitutive relations for stresses and couple stresses can be represented as linear tensor-valued functions of strain $\varepsilon_{ij}=u_{j,i}-e_{ijn} \theta_n$, $\kappa_{ij}=\theta_{j,i}$. For micropolar elasticity we modified the Voigt notation as follows

$$\{\sigma_M\} = [C]\{\varepsilon_M\}, \quad [C] = \begin{bmatrix} \mathbf{A} & \mathbf{0} \\ \mathbf{0} & \mathbf{B} \end{bmatrix}, \quad \{\sigma_M\} = \begin{bmatrix} \mathbf{T} \\ \mathbf{M} \end{bmatrix}, \quad \{\varepsilon_M\} = \begin{bmatrix} \mathbf{E} \\ \mathbf{K} \end{bmatrix}, \quad (3)$$

where

$$\{\mathbf{T}\} = \{t_{11}, t_{22}, t_{33}, t_{12}, t_{21}, t_{23}, t_{32}, t_{13}, t_{31}\}^T, \quad (4)$$

$$\{\mathbf{M}\} = \{m_{11}, m_{22}, m_{33}, m_{12}, m_{21}, m_{23}, m_{32}, m_{13}, m_{31}\}^T, \quad (5)$$

$$\{\mathbf{E}\} = \{\varepsilon_{11}, \varepsilon_{22}, \varepsilon_{33}, \varepsilon_{12}, \varepsilon_{21}, \varepsilon_{23}, \varepsilon_{32}, \varepsilon_{13}, \varepsilon_{31}\}^T, \quad (6)$$

$$\{\mathbf{K}\} = \{\kappa_{11}, \kappa_{22}, \kappa_{33}, \kappa_{12}, \kappa_{21}, \kappa_{23}, \kappa_{32}, \kappa_{13}, \kappa_{31}\}^T, \quad (7)$$

with 18×18 stiffness matrix $[C]$, 9×9 matrices \mathbf{A} and \mathbf{B} which are not shown here. The exact form of $[C]$ is given in Eremeyev and Pietraszkiewicz (2016), Eremeyev et al. (2013), Eremeyev et al. (2016a).

In what follows we implement the micropolar elastic constitutive equations in ABAQUS. Details of the implementation including the description of the user defined 8-node hybrid micropolar isoparametric element, stiffness matrix, etc, are given by Eremeyev et al. (2016a). Here we are concentrated on the visualization of obtained results.

3. Visualization of the user elements results

Application of user elements in the commercial software requires additional tasks in order to visualize the obtained results. In ABAQUS program (used in the presented research) user elements are represented by nodes only. ABAQUS does not recognize the user element faces or volumes. The 2D element defined by four nodes presented in Fig. 1a. can be treated as the rectangular 2D solid (Fig. 1b), as the 2D frame consisting of beam elements (Fig. 1c) or as the 2D truss bar structure (Fig. 1d).

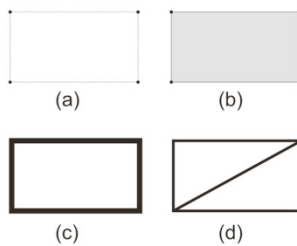


Fig. 1. Various representations of the user element.

Because of this ambiguous user element representation there are some limitations in application of user elements in ABAQUS software, e.g. the pressure cannot be applied to the face, the contact face-to-face is not allowed etc. Some serious problems arise in the visualization of the obtained results as well. The finite element mesh consisting of ordinary elements shown in Fig. 2(top) in the case of user elements can be represented by nodes only (Fig. 2bottom).

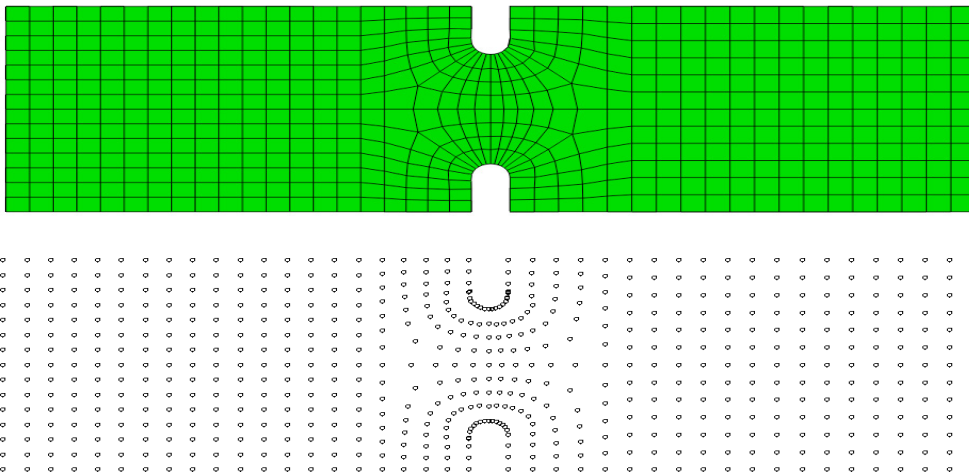


Fig. 2. Graphical representation of ordinary elements (above) and user elements (below).

The only possible visualization of the user elements results is the vector plot of nodal displacements shown in Fig.3.

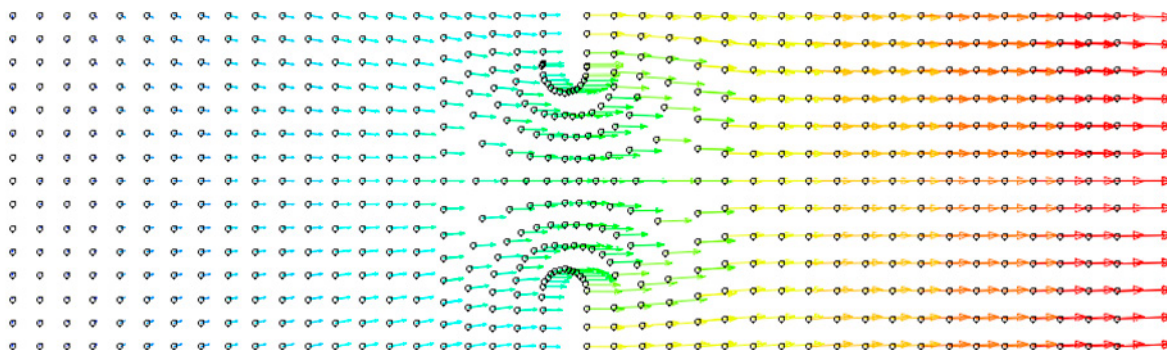


Fig. 3. Nodal displacements of user elements.

In this research to visualize the stress distribution in continuous 3D user elements two different approaches are recommended.

In the first approach the 3D graphical program based on OpenGL library have been developed (see Wright and Sweet, 1996). This is a very ambitious task which requires high-level programming skill in Microsoft Foundation Class (MFC) and OpenGL libraries. The OpenGL library allows for writing very effective code to display sophisticated 3D graphics which is being accelerated by the hardware. Such features as: 3D space transformations, depth buffer, color and shading, lighting and lamps, double buffering etc. allow the programmer to concentrate on crucial part of the numerical code without going into technical details about the hardware. In practice, own graphical programs may be more comfortable than the commercial ones mostly because they can be easily modified according to the user needs.

In the second approach the special Python script is developed for the ABAQUS visualization module. In ABAQUS program all the user activities resulting from menu, trees or dialog boxes actions are exchanged into appropriate Python commands executed by the ABAQUS kernel. The ABAQUS engineers have been extended the standard Python script language by numerous ABAQUS objects. In the case of postprocessor the following objects are available: output database, part, material, section, type of analysis, finite elements, boundary conditions, displacements, stress tensor and many others. These objects own their data and methods which operate on these data. Thus, the method which saves the output database object to the binary file, forces saving to this file all postprocessor objects (mentioned above) created by the Python script. This way fully-functioning output database is made which does not differ from the database generated by the ABAQUS solver. This task requires good knowledge of object-oriented programming (in particular Python language), and good knowledge of ABAQUS objects. The advantage of this approach is that all the ABAQUS visualization module features are available for the user. Similar but less effective technique to visualize results of user elements has been implemented by Roth et al., where the results obtained for ABAQUS built-in elements have been replaced by the Python script by the results of user elements.

4. Benchmark tests

As the benchmark test the contact between cylinder and two flat plates is considered. Because of the problem symmetry only one plate and the half of the cylinder is considered. Both parts are meshed by hexahedral or by tetrahedral linear finite elements. The cylinder is meshed by user elements developed for micropolar approach while the plate is meshed by ABAQUS built-in 3D finite elements. The nodes-to-surface contact is assumed. The FEM mesh consisting of tetrahedral elements is shown in Fig. 4.

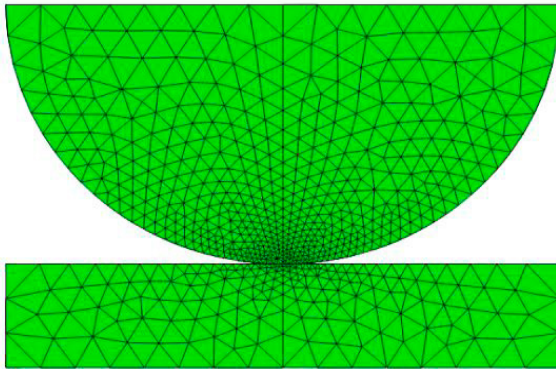


Fig. 4. FEM mesh – tetrahedral elements.

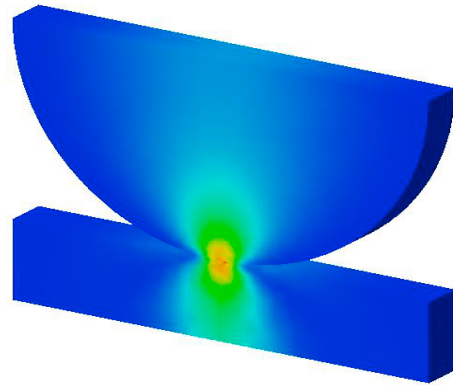


Fig. 5. Von Mises stress distribution – developed software.

The distribution of von Mises stress presented in developed graphical program based on OpenGL library is presented in Fig.5.

The distribution of von Mises stress displayed in ABAQUS visualization module is shown in Fig.6. Here, the mirror operation is applied to present the whole model (in computations because of the problem symmetry only half of the model have been used).

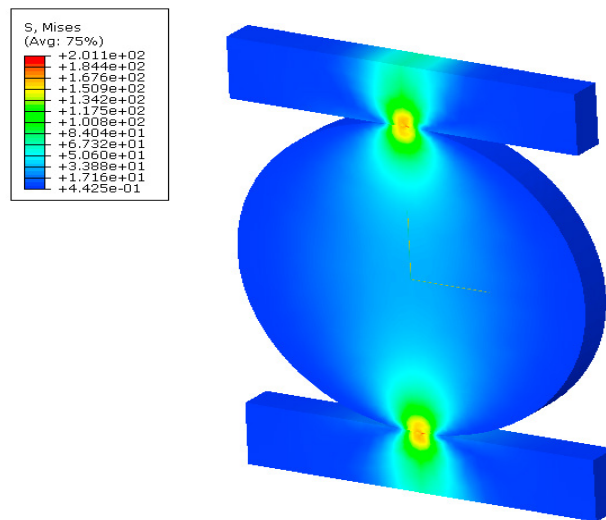


Fig. 6. Von Mises stress distribution [MPa]– ABAQUS visualization module.

Comparison of visualizations presented in Fig. 5 and Fig. 6. shows an excellent compatibility of this two types of graphical programs. In Fig. 7 the distribution of m_{yy} stress is presented – in ABAQUS visualization module only half of cylinder is displayed.

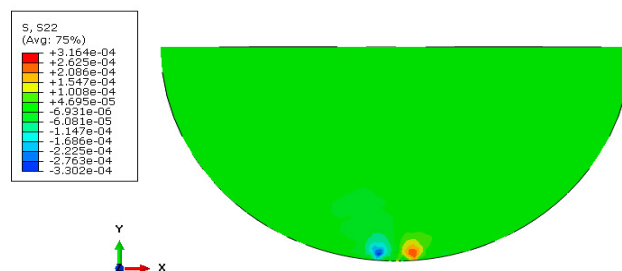


Fig. 7. m_{yy} stress distribution [MN/m].

4. Conclusions

Here we discuss the implementation of new 8-node hybrid micropolar isoparametric element in ABAQUS in order to model the behavior of microstructured materials. We presented the solutions of few 3D benchmark problems of the micropolar elasticity including contact ones and the problems with notches. Comparison of classical and micropolar solutions shown that couple stress appears almost in the vicinity of singularities that is near notches and contact areas. Using the discussed here technique we extend the preliminary results on the modeling of bioceramic implants in bones performed by Eremeyev et al. 2016b.

Acknowledgements

Authors acknowledge the support by the People Program (Marie Curie Curie ITN transfer) of the European Union's Seventh Framework Programme for research, technological development and demonstration under grant agreement No PITN-GA-2013-606878.

References

- Eremeyev, V.A., Lebedev, L.P., Altenbach, H., 2013. Foundations of Micropolar Mechanics. Springer, Heidelberg et al.
- Eremeyev, V.A., Pietraszkiewicz, W., 2016. Material symmetry group and constitutive equations of micropolar anisotropic elastic solids. *Math. Mech. Solids* 21(2), 210–221
- Eremeyev, V.A., Pietraszkiewicz, W., 2012. Material symmetry group of the non-linear polar-elastic continuum. *Int. J. Solids Struct.* 49(14), 1993–2005
- Eremeyev, V. A., Skrzat, A., Stachowicz, F., 2016a. On finite element computations of contact problems in micropolar elasticity. *Advances in Materials Science and Engineering*. 2016. Article ID 9675604, 1-9.
- Eremeyev, V. A., Skrzat, A., Vinakurava, A. 2016b. Application of the micropolar theory to the strength analysis of bioceramic materials for bone reconstruction. *Strength of Materials*, 48(4), 573-582
- Eringen, A.C.: *Microcontinuum Field Theory. I. Foundations and Solids*. Springer, New York (1999)
- Goda, I., Ganghoffer, J.F., 2015. Identification of couple-stress moduli of vertebral trabecular bone based on the 3d internal architectures. *J. Mech. Behavior Biomed. Materials* 51, 99–118
- Lakes, R., 1986. Experimental microelasticity of two porous solids. *Int. J. Solids Struct.* 22(1), 55–63
- Liebold, C., Müller, W. H., 2015. Are Microcontinuum Field Theories of Elasticity Amenable to Experiments? A Review of Some Recent Results. In *Differential Geometry and Continuum Mechanics* (pp. 255-278). Springer International Publishing.
- Roth, S., Hütter, G., Mühlich, U., Nassauer, B., Zybelle, L., Kuna, M. Visualisation of User Defined Finite Elements with ABAQUS/Viewer, gaCMReport <http://tu-freiberg.de>
- Trovalusci, P., Ostojca-Starzewski, M., De Bellis, M.L., Murrall, A. 2015. Scale-dependent homogenization of random composites as micropolar continua. *Eur. J. Mech. A/Solids* 49, 396–407.
- Wright, R., Sweet, M., 1996. *OpenGL Super Bible*, Wait Group Press, Corte Madera.
- Yang, J., Lakes, R.S., 1982. Experimental study of micropolar and couple stress elasticity in compact bone in bending. *J. Biomechanics* 15(2), 91–98.